Journal of Photochemistry and Photobiology A: Chemistry 207 (2009) 135–143

Contents lists available at ScienceDirect

Journal of Photochemistry and Photobiology A: Chemistry

journal homepage: www.elsevier.com/locate/jphotochem

Photocatalytic electron flow through the interface of titania nanosheets and mesoporous silica hybrid films

Tatsuto Yui[a,b], Takuya Hirano[a], Ken-ichi Okazaki[a,b], Haruo Inoue[c], Tsukasa Torimoto[a,**], Katsuhiko Takagi[a,c,d,*]

[a] Department of Crystalline Materials Science, Graduate School of Engineering, Nagoya University, Chikusa-ku, Nagoya 464-8603, Japan
[b] CREST (JST), Japan
[c] Department of Applied Chemistry, Tokyo Metropolitan University, Minami-ohsawa, Hachiohji, Tokyo 192-0397, Japan
[d] Kanagawa Academy of Science and Technology, Sakato 3-2-1, Takatsu-ku, Kawasaki, Kanagawa 213-0012, Japan

ARTICLE INFO

Article history:
Available online 25 December 2008

Keywords:
Charge separation
Photocurrents
Electron transfer
Nanosheet
Mesoporous silica
Organic–inorganic hybrids
Porphyrin
Viologen

ABSTRACT

UV-light induced redox reactions between cationic porphyrins (H_2TMPyP) and methyl viologen (MV^{2+}) separately incorporated in titania nanosheets (TNS) and *cubic*-mesoporous silica (MPS) integrated films, respectively, were investigated. In this system, the following two modified hybrids, *i.e.*, the normally stacked (MV^{2+}–TNS)/(H_2TMPyP–MPS) on a FTO electrode and the inversely stacked (H_2TMPyP–MPS)/(TNS) films on a FTO electrode were examined. In accordance with the expected electron flow from H_2TMPyP to MV^{2+}, cathodic photocurrents were observed for the normally stacked film in acetonitrile (CH_3CN) under a negative bias voltage of −0.4 V. However, under the influence of a positive bias voltage of +0.3 V, anodic photocurrents were observed even in CH_3CN. On the other hand, anodic photocurrents were also observed in water for the normally stacked films at both bias voltages of +0.3 and −0.4 V due to photoreduction followed by proton abstraction of the H_2TMPyP molecules from H_2O within the MPS nano-cavities. In addition, *ca.* 0.98 mC of the photocurrents were determined in water for the inversely stacked (H_2TMPyP–MPS)/(TNS) films without MV^{2+}, of which *ca.* 50% resulted in the oxidative consumption of H_2TMPyP in the MPS cavities.

1. Introduction

The hybridization of organic guest molecules within nanostructured cavities of inorganic host materials has been the focus of recent investigations [1–3] using zeolites [4], clay minerals [5–7], mesoporous silicas [8], and layered metal oxides [1–3,9–10]. From a photochemical and photophysical perspective, such hybrids are intriguing due to the unique and characteristic photofunctionality of the intercalated organic molecules [1–5,8]. Highly efficient and selective reactions are possible through such properties as anisotropic control due to the structural orientation [11–14], improvement in the lifetime of the nonpersistent species [15–22], and the acceleration of various photochemical reactions [23,24]. The photochemical properties of layered metal oxide semiconductors (LMOSs), such as layered niobate [25–27], titanate [28–33], and their exfoliated materials [1,3,28,29], are especially interesting for their photocatalytic properties [34] and intercalation characteristics [1–3].

In our previous work [35–39], consecutively stacked hybrid thin films of *cubic*- [40] or spherical-structured [41] mesoporous silica (MPS) films and layered titania nanosheets (TNS) [28–32] were shown to exhibit unique interactions between the *tetra*-pyridinium-porphyrins (H_2TMPyP) with methyl viologen (MV^{2+}). In these stacked hybrid films, H_2TMPyP and the electron-accepting MV^{2+} were separately accommodated within the nano-cavities of *cubic*-MPS and the interlayers of the photocatalytic TNS, respectively [35]. The (MV^{2+}–TNS) film was coated on the (H_2TMPyP–MPS) film to form consecutively stacked hybrids, i.e., a (MV^{2+}–TNS)/(H_2TMPyP–MPS) hybrid film exhibiting photo-induced electron transfers through their heterogeneous interface [35–37]. Upon UV-light irradiation of the TNS within the (MV^{2+}–TNS)/(H_2TMPyP–MPS) hybrid films, one-electron reduced radical ions ($MV^{+\bullet}$) of MV^{2+} were formed, accompanied by the oxidative consumption of H_2TMPyP ions and resulting in a charge separation (CS) at the interface of the stacked hybrid films of the two types of inorganic host materials. Interestingly, the CS within the TNS/MPS hybrids occurred reversibly, surviving even under ambient conditions and being retained even after standing for several

* Corresponding author at: Kanagawa Academy of Science and Technology, Sakato 3-2-1, Takatsu-ku, Kawasaki, Kanagawa 213-0012, Japan.
** Corresponding author at: Department of Crystalline Materials Science, Graduate School of Engineering, Nagoya University, Chikusa-ku, Nagoya 464-8603, Japan.
E-mail addresses: torimoto@apchem.nagoya-u.ac.jp (T. Torimoto), k-takagi@newkast.or.jp (K. Takagi).

1010-6030/$ – see front matter © 2009 Elsevier B.V. All rights reserved.
doi:10.1016/j.jphotochem.2008.12.018

hours [39]. The photochemical behavior and electron pathways of the (MV^{2+}–TNS)/(H_2TMPyP–MPS) hybrid film are summarized as follows in Eqs. (1)–(3).

$$\mathrm{TNS} + \text{UV-light} \rightarrow e^-_{cb} + h^+ \quad (1)$$

$$e^-_{cb} + MV^{2+}\,(\text{in TNS}) \rightarrow MV^{+\bullet}\,(\text{in TNS}) \quad (2)$$

$$h^+ + H_2\text{TMPyP}\,(\text{in MPS}) \rightarrow [H_2\text{TMPyP}]_{ox}\,(\text{in MPS}) \quad (3)$$

where e^-_{cb}, h^+, and $[H_2\text{TMPyP}]_{ox}$ denote the electrons in the conduction band, holes in the valence band of TNS, and the oxidation products of H_2TMPyP, in this order, respectively. Judging from the proposed reaction pathways, the e^-_{cb} or h^+ is expected to migrate through the TNS/MPS interface and the photo- and electrochemically inert MPS nano-cavities [35]. For the single-coated *cubic*-MPS transparent films, *i.e.*, the (H_2TMPyP–MPS) films on a FTO electrode, it was reported that the photo-generated electrons/holes may migrate even in the photo- and electrochemically inert MPS nano-cavities with a thickness of *ca.* 0.5 μm [42]. This suggests that the electrons and holes migrate even in the double-coated (MV^{2+}–TNS)/(H_2TMPyP–MPS) films, although electron/hole migrations within the entire (MV^{2+}–TNS)/(H_2TMPyP–MPS) films have yet to be reported. Here, we will report on the preparation of double-coated (MV^{2+}–TNS)/(H_2TMPyP–MPS) films on a FTO electrode and the observation of electron migrations through the TNS/MPS interface initiated by photo- and electrochemical techniques.

2. Experiments

2.1. Materials

The preparation of a proton-exchanged layered titanate ($H_{0.7}Ti_{1.825}O_4{\cdot}H_2O$) and its exfoliation was carried out by experimental procedures previously reported by Sasaki et al. [28–32]. A 1.2 wt% aqueous dispersed solution of titania nanosheets (TNS) exfoliated by the addition of 0.03 M tetrabutylammonium hydroxide (TBA^+OH^-) were prepared. Aqueous dispersions of 4.15 cm^3 exfoliated TNS (12 g dm^{-3}), aqueous solution of 2.28 cm^3 poly(vinylalcohol) (PVA: 10 g dm^{-3}), and water (4.97 cm^3) was stirred for 5 days at ambient temperature [22].

1,1′-Dimethyl-4,4′-bipyridinium dichloride (MV^{2+} $2Cl^-$; TCI), α,β,γ,δ-*tetrakis* (1-methylpyridinium-4-yl)porphyrin *p*-toluenesulfonate (H_2TMPyP, TCI), PVA (TCI, DP ~2000), tetramethoxysilane (TMOS; TCI) and cetyltrimethylammonium chloride (CTAC; TCI) of extra pure grade were used without further purification. The water was purified by UV treatment and de-ionization processes (Elix UV-5; Millipore Japan). The remaining chemical reagents and materials were of extra pure grade and used without further purification.

2.2. Preparation of TNS and MPS hybrid films

Two different nano-structured inorganic films, a titania nanosheet (TNS) and *cubic*-structured mesoporous silica film (MPS), were deposited on a 40 mm × 40 mm F-doped SnO_2 glass (FTO; Asahi Grass, Sheet Resistance: 10 Ω squire^{-1}) electrode by two different stacking procedures, as shown in Fig. 1, i.e., (a) (MV^{2+}–TNS) was cast on a (H_2TMPyP–MPS) film; and (b) (H_2TMPyP–MPS) was cast on a TNS film. In case (b), the hybrid film was covered with a thin Nafion film so that the H_2TMPyP would not dissolve into the aqueous bulk solution. The resulting two transparent hybrid thin films were used for photo-electrochemical investigations. The FTO electrodes were used after washing well with acetone just before use.

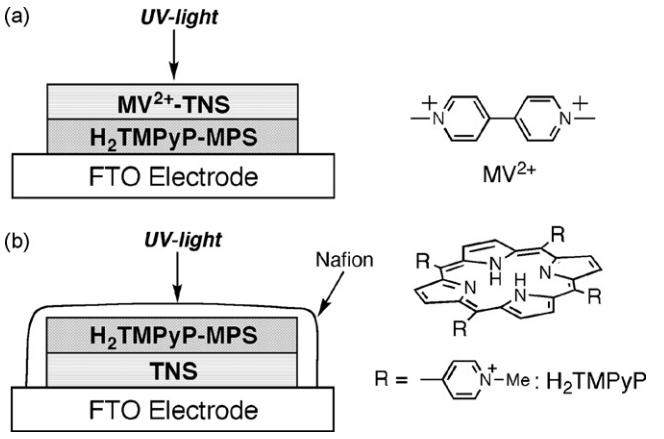

Fig. 1. Schematic structure of two types of hybrid films each on a FTO electrode: (a) normally stacked (MV^{2+}–TNS)/(H_2TMPyP–MPS) hybrid films; and (b) inversely stacked (H_2TMPyP–MPS)/(TNS) hybrid films.

2.2.1. Normally stacked (MV^{2+}–TNS)/(H_2TMPyP–MPS) hybrid films

The (MV^{2+}–TNS)/(H_2TMPyP–MPS) hybrid films were prepared according to procedures somewhat modified from that of previous literature [35]. An aqueous MPS precursor gel suspension including TMOS and CTAC was spin-coated (3000 rpm, 10 s) on a FTO electrode and then calcined at 350 °C for 3 h [40]. The MPS films on the FTO were soaked for 1 min in methanolic solution of 0.1 wt% NaOH and washed well with methanol [35]. The obtained thin films were soaked for 1.0 h in 10 mL aqueous solution of 1.0×10^{-4} M H_2TMPyP at ambient temperature, leading to the formation of brownish-colored (H_2TMPyP–MPS) films. The (H_2TMPyP–MPS) films were then coated with a TNS film by casting a TNS aqueous dispersion on the MPS film, followed by soaking in an aqueous 2.0×10^{-4} M solution of MV^{2+} for 4 h at ambient temperature and drying under ambient atmosphere. The obtained (MV^{2+}–TNS)/(H_2TMPyP–MPS) hybrid films were structurally analyzed by X-ray diffraction (XRD) as well as electronic absorption spectroscopy [35]. Scanning electron micrograph (SEM) clearly showed the surface and interface of the (MV^{2+}–TNS)/(H_2TMPyP–MPS) hybrid films to have uniform and smoothly stacked structures. The thickness of the TNS and MPS films were estimated to be *ca.* 0.5 and 0.8 μm, respectively, as shown in Fig. 2a. No physical contact between the TNS film and FTO electrode was confirmed for the (MV^{2+}–TNS)/(H_2TMPyP–MPS)/FTO film since a short circuit could not be observed between the TNS and FTO films.

2.2.2. Inversely stacked (H_2TMPyP–MPS)/(TNS) hybrid films

An aqueous dispersed solution of the TNS was cast on a FTO electrode and the deposited TNS films were dried at 200 °C for 1.0 h. An aqueous suspension of the MPS precursor gel with TMOS and CTAC was spin-coated on the TNS films and then calcined at 200 °C for 10 h to form the (MPS)/(TNS) films. The obtained (MPS)/(TNS) films were then treated with an NaOH solution, as has been described. The transparent thin films were soaked for 1.0 h in a 1.0×10^{-4} M aqueous solution of H_2TMPyP at ambient temperature, thus, forming the (H_2TMPyP–MPS)/(TNS) hybrid films. To avoid desorption of the H_2TMPyP within the MPS nano-cavities into the electrolyte solution, a 5 wt % aqueous solution of Nafion (adjusted to pH 7 with NaOH) was spin-coated (3000 rpm, 10 s) on the hybrid film. The resulting (H_2TMPyP–MPS)/(TNS) hybrid films were then analyzed by XRD and absorption measurements [35]. A clear layered structure consisting of the [MPS–TNS-FTO] layers was confirmed by SEM observations, the thicknesses of which were estimated to be 2 and 0.2 μm for the TNS and MPS, respectively, as shown in Fig. 2b.

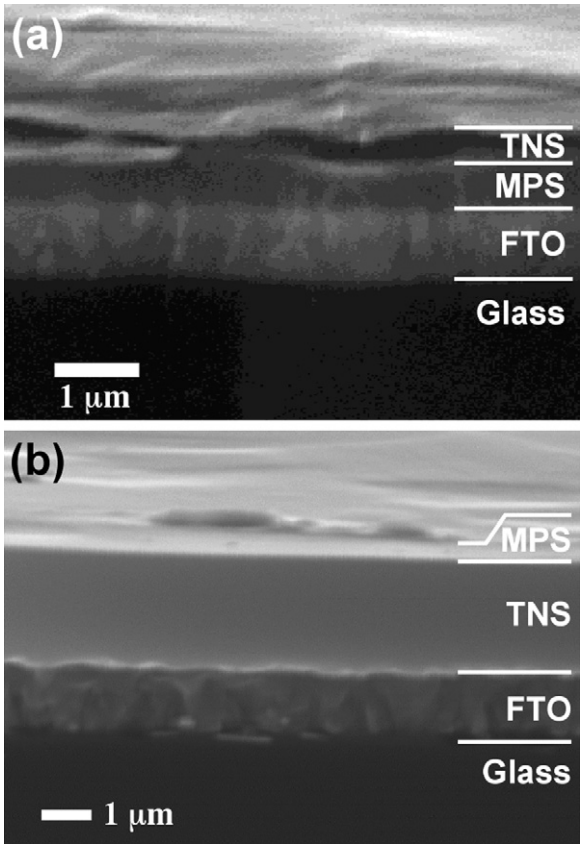

Fig. 2. Cross-sectional SEM image of: (a) normally stacked (MV^{2+}–TNS)/(H_2TMPyP–MPS); and (b) inversely stacked (H_2TMPyP–MPS)/(TNS) hybrid films on the FTO electrode.

The selective adsorption of H_2TMPyP into the MPS nano-cavities of the normally or inversely stacked films were confirmed by absorption measurements. When the H_2TMPyP molecules were intercalated within the stacked layered materials, a 50–60 nm red-red shift of its Soret absorption spectrum as compared to that in aqueous solution was observed due to the gradual flattening of the methyl-pyridinium rings against porphyrin rings [13,14]. The absorption maxima of the H_2TMPyP in the various systems are summarized in Table 1 and it can be seen that H_2TMPyP possesses an absorption maximum at 430–435 nm in the MPS nano-cavities for all the systems (b)–(d) with a red-shift of 9–14 nm, as compared to the Soret absorption band in aqueous solution. The Soret band maxima of the porphyrins are known to be sensitive to the polarity of the solvent used, *i.e.*, in a less polar solvent environment, the absorption maximum shifts toward red [43]. The observed red-shift indicates a decrease in the environmental polarity within the MPS nano-cavities. However, when the H_2TMPyP molecules were intercalated into the stacked layered material (systems e or f), the Soret bands were significantly red-shifted due to flattening [13,44,45], as compared to the MPS nano-cavities. These results clearly show that the H_2TMPyP molecules were efficiently adsorbed into the MPS nano-cavities but not into the TNS interlayers.

Table 1
Soret absorption maxima of H_2TMPyP in various systems.

System	λ_{max} (nm)
(a) Aqueous solution	421
(b) (H_2TMPyP–MPS)	430
(c) (MV^{2+}–TNS)/(H_2TMPyP–MPS)	433
(d) (H_2TMPyP–MPS)/(TNS)	435
(e) (H_2TMPyP–TNS)[a]	475
(f) Intercalation in clay layer[b]	484

[a] Reported values in ref. [35].
[b] Reported values in ref. [13].

2.3. Electrochemical studies under UV-light illuminations

A three-electrode cell composed of the FTO coated with the hybrid films, Pt, and the Ag/AgCl (satd. KCl) as the action, counter, and reference electrodes, respectively, was used for electrochemical analysis under UV-light illumination [42]. Circle-shaped quartz windows of Ø 50 mm were equipped on both sides of the cell. One-hundred millimolars of the aqueous Na_2SO_4 solution or 10 mM $LiClO_4$ acetonitrile solution was used as the electrolyte solution under N_2 gas atmosphere. The applied voltage was controlled by a potentiostat/galvanostat instrument (HOKUTO H-105) and function generator (HOKUTO H-301). A 300 W Xe lamp (USHIO X300) was used as the light source together with U-340 and IRA 25S filters (HOYA) for UV-light irradiation of 300–380 nm with a light intensity of 0.02 W cm^{-2}. Both the normally and inversely stacked films were irradiated by UV-light from the TNS/MPS hybrid film side, as shown in Fig. 1. The Xe lamp was also used as a probe light source for spectral measurements of the sample films together with a USB2000 (Ocean Optics) detector.

2.4. Equipment

The UV–visible absorption spectra were recorded on a JASCO spectrometer, type V-550, generally in transmittance mode. The scanning electron micrograph (SEM) images were recorded on a JSM-5600 apparatus (JEOL) operating at 20 kV for the Au-coated samples. Powder X-ray diffraction analysis (XRD) was carried out with a Rigaku RINT-2100 XRD apparatus operating at 40 kV and 40 mA and set at Ni-filtered CuK_α radiation of 0.154 nm wavelength.

3. Results and discussions

3.1. Redox characteristics without light irradiation

Electrochemical analysis of H_2TMPyP in the MPS/TNS hybrid films was performed in aqueous and non-aqueous solutions under dark conditions [42]: The current–voltage (V–A) profiles of H_2TMPyP for the hybrid films on the FTO electrode exhibited two negative currents at *ca.* −0.3 and −0.6 V in an aqueous Na_2SO_4 solution under dark, which corresponded to the formation of two kinds of reduced species from H_2TMPyP, i.e., a two-electron reduced species followed by a two-proton attached H_2TMPyP [P(-II)H_4], and a one-electron reduced anion radical [P(0)$H_2^{-\bullet}$], respectively. Neri and Wilson have reported that three negative currents at −0.29, −0.53 and −0.62 V (vs. Ag/AgCl) are observed in the electro-reduction of an aqueous H_2TMPyP solution under acidic to neutral conditions [46]. Here, the former two peaks were assigned to P(-II)H_4 and the further reduced species ($[P(-VI)H_{(4+n)}]^{(n-4)-}$), respectively, and the latter corresponded to P(0)$H_2^{-\bullet}$, as shown in Scheme 1(a and b), respectively [42]. Here, $[P(-VI)H_{(4+n)}]^{(n-4)-}$ is tentatively assigned to the six-electron reduced porphyrin or its homologs with eight protons ($4+n=8$) [46]. The protonated species, thus, tend to decrease while the non-protonated species increases with an increase in the pH from 0 to 6. In fact, no negative current at *ca.* −0.5 V was observed, probably due to the small number of protons below the detection limit under neutral conditions. In addition, no appreciable redox currents from the H_2TMPyP were observed in the range of a more positive voltage from −0.2 to +0.8 V.

Similar current–voltage profiles were taken with the (MV^{2+}–TNS)/(H_2TMPyP–MPS) hybrid films in non-hydroxylic

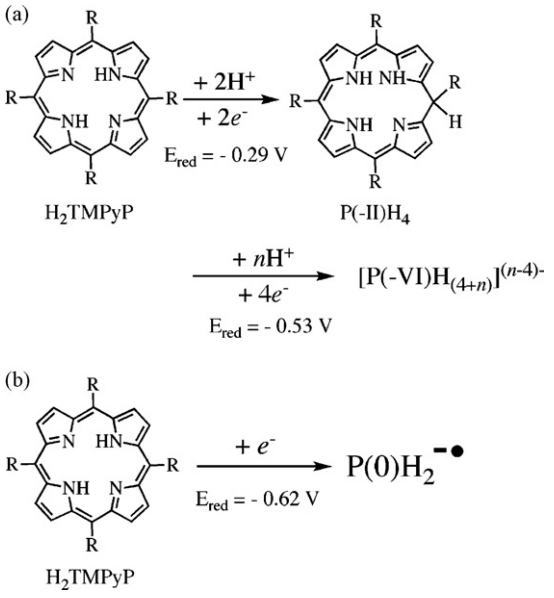

Scheme 1. Electrochemical reduction mechanisms of H_2TMPyP under dark conditions in: (a) hydroxylic and; (b) non-hydroxylic solvents.

polar solvents such as CH_3CN, as exemplified in Fig. 3. A clear reduction signal was observed at −0.64 V, indicating the formation of $P(0)H_2^{-\bullet}$ without any redox signals at regions of −0.5 to +0.5 V. These results clearly indicate that no protonated species such as $P(-II)H_4$ or $[P(-VI)H_{(4+n)}]^{(n-4)-}$ were formed at all in non-hydroxylic solvents (Scheme 1b).

3.1.1. (H_2TMPyP–MPS) films in aqueous solution

Upon visible light irradiation of the half-stacked hybrid films (H_2TMPyP–MPS) on the FTO electrode, both anodic and cathodic photocurrents were observed under an applied bias voltage (V_a) of either positive (+0.3 V) or negative (−0.4 V), respectively [42]. These results indicate the direction in which the electrons flow in the hybrid films are affected by the applied bias voltage (V_a).

3.1.2. (MV^{2+}–TNS)/(H_2TMPyP–MPS) films in aqueous solution

In a similar manner, UV-light irradiation was carried out at a bias voltage of +0.3 or −0.4 V for the double-coated hybrid films (MV^{2+}–TNS)/(H_2TMPyP–MPS) upon UV-light irradiation in aqueous solutions.

3.1.2.1. V_a = +0.3 V. The absorption spectral changes of the (MV^{2+}–TNS)/(H_2TMPyP–MPS) hybrid films under UV-light irradiation at an applied voltage of (V_a) = +0.3 V are shown in Fig. 4a. Thus, the Soret absorption band of H_2TMPyP at 430 nm decreased with the simultaneous generation of considerable anodic photocurrents (Fig. 4a, inset). Moreover, new absorption bands at around 520 nm appeared. This implies the formation of two-electron reduced H_2TMPyP ($P(-II)H_4$) [46], which remains in the MPS nano-cavities even after UV-light irradiation of 60 min. These results suggest that the photo-generated e_{cb}^- reduces the H_2TMPyP in the MPS nano-cavities, forming $P(-II)H_4$, followed by a migration to the FTO electrode. However, the absorption maxima at *ca.* 380 nm for $MV^{+\bullet}$ did not increase even under UV-light irradiation due to the preferential reduction of H_2TMPyP over MV^{2+}.

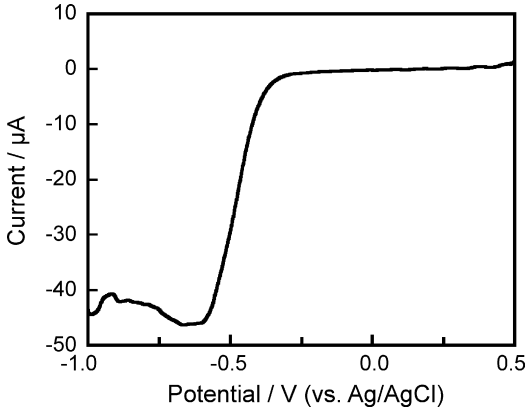

Fig. 3. Current–voltage (V–A) profile of the (MV^{2+}–TNS)/(H_2TMPyP–MPS) hybrid films on a FTO electrode in CH_3CN in the dark.

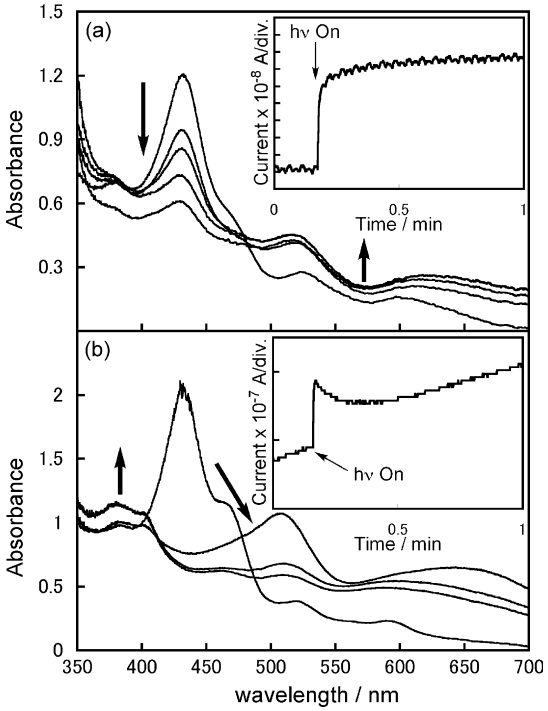

Fig. 4. Changes in the absorption spectra for the normally stacked (MV^{2+}–TNS)/(H_2TMPyP–MPS) hybrid films on a FTO electrode in aqueous solution with: (a) positively applied voltage (+0.3 V) and UV-light irradiation of 0, 10, 20, 40, 60 min; and (b) negatively applied voltage (−0.4 V) and UV-light irradiation of 0, 10, 30, 40 min. Insets show photocurrent generation for the (MV^{2+}–TNS)/(H_2TMPyP–MPS) hybrid films on the FTO electrode.

3.1.2.2. V_a = −0.4 V. The absorption spectra of the (MV^{2+}–TNS)/(H_2TMPyP–MPS) hybrid films under UV-light irradiation with an applied voltage of (V_a) = −0.4 V are shown in Fig. 4b. UV-light irradiation led to a decrease in the Soret absorption band of H_2TMPyP at 430 nm, simultaneously accompanied by the generation of considerable anodic photocurrents (Fig. 4b, inset). In contrast to the positive voltage of V_a = +0.3 V, new absorption bands at *ca.* 380 and 650 nm corresponding to $MV^{+\bullet}$ newly appeared. In addition, the Soret absorption band bathochromically shifted to *ca.* 500 nm within the initial 10-min UV-light irradiation, which then decreased after prolonged irradiation of 60 min. This suggests that the H_2TMPyP molecules were reduced to $P(-II)H_4$ in the MPS nano-cavities during the initial stage and its further multi-electron reduction resulted in successive decomposition [46]. The reduction of the H_2TMPyP molecules in the MPS nano-cavities are competitively reduced with those of MV^{2+} within the interlayer of TNS under conditions of negative voltage (V_a = −0.4 V).

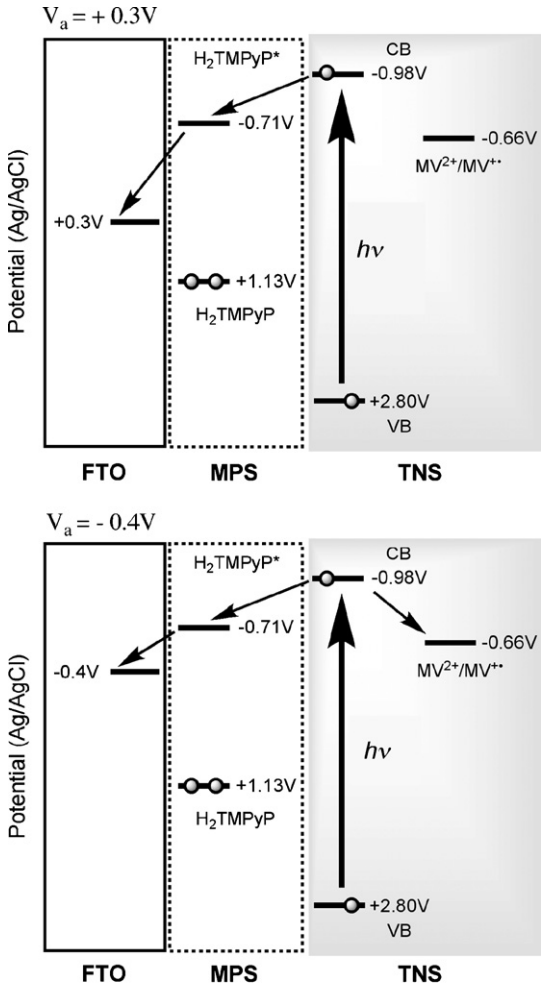

Scheme 2. Proposed schemes for the electron flow in the normally stacked (MV^{2+}–TNS)/(H_2TMPyP–MPS) hybrid films on a FTO electrode in aqueous solution with applied positive (+0.3 V) and negative (−0.4 V) bias voltages.

On the basis of these results, electron migration mechanisms could be proposed for the normally stacked (MV^{2+}–TNS)/(H_2TMPyP–MPS) hybrid films in aqueous systems, as shown in Scheme 2. By applying a positive bias voltage, only H_2TMPyP in MPS was reduced accompanied by the generation of anodic photocurrents, however, both H_2TMPyP in MPS and MV^{2+} in TNS were reduced with the generation of anodic photocurrents in the case of a negative bias voltage. An anodic photocurrent was generated in the normally stacked (MV^{2+}–TNS)/(H_2TMPyP–MPS) hybrid films with an applied voltage of V_a = −0.4 V in aqueous solutions, which was in sharp contrast with the half-stacked (H_2TMPyP–MPS) films [42] or other hybrid systems, as described below.

3.2. Normally stacked (MV^{2+}–TNS)/(H_2TMPyP–MPS) films in CH_3CN

In aqueous solutions, the formation of P(-II)H_4 molecules in the MPS nano-cavities occurred prior to the oxidation of H_2TMPyP and reduction of MV^{2+}. No detectable currents were observed for the normally stacked (MV^{2+}–TNS)/(H_2TMPyP–MPS) hybrid films in non-hydroxylic solvents, *e.g.*, CH_3CN under dark in −0.5 to +0.8 V regions, as shown in Fig. 2. However, the normally stacked (MV^{2+}–TNS)/(H_2TMPyP–MPS) hybrid films underwent UV-light induced electron transfers in CH_3CN.

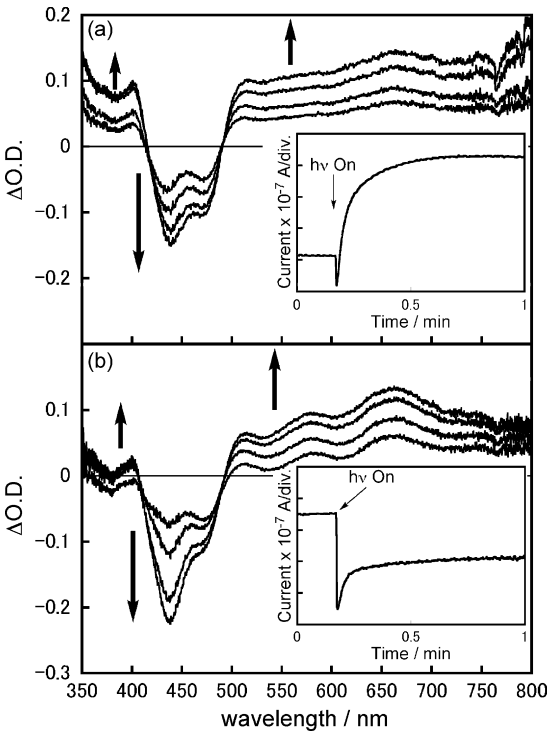

Fig. 5. Changes in the differential absorption spectra for the normally stacked (MV^{2+}–TNS)/(H_2TMPyP–MPS) hybrid films on a FTO electrode in acetonitrile solution with: (a) positive (+0.3 V); and (b) negative (−0.4 V) applied voltages under 0, 10, 20, 40, and 60 min UV-light irradiation. Inset shows the photocurrents generated with the normally stacked (MV^{2+}–TNS)/(H_2TMPyP–MPS) hybrid films on the FTO electrode.

3.2.1. Photoreactions for V_a = +0.3 V

Changes in the differential absorption spectra for the (MV^{2+}–TNS)/(H_2TMPyP–MPS) hybrid films under UV-light irradiation with an applied voltage of (V_a) = +0.3 V in CH_3CN are shown in Fig. 5a. Upon UV-light irradiation, the Soret absorption band of H_2TMPyP at 430 nm decreased with simultaneous photocurrent generation (Fig. 5a, inset). In contrast to aqueous solution systems, the formation of one-electron reduced MV^{2+}, *i.e.*, $MV^{+\bullet}$, was confirmed by the characteristic absorption bands at *ca.* 390 and 500–700 nm without the reduction of H_2TMPyP, implying that the reductions of the H_2TMPyP molecules in the MPS nano-cavities were suppressed by the preferential reduction of the MV^{2+} molecules in TNS. Hence, a cathodic current was observed within the initial few seconds, although the direction for the flow of the photocurrents gradually changed from a cathodic to an anodic upon prolonged UV-light irradiation. These results imply that the reduction of MV^{2+} in TNS by e^-_{cb}, the oxidation of H_2TMPyP in MPS by h^+, and the electron injection from the FTO electrode to the oxidized H_2TMPyP occurred at the initial stage of the photochemical activity. However, upon prolonged light irradiation, the photochemical reduction of H_2TMPyP occurred preferentially to MV^{2+} and induced the anodic currents towards opposite directions. In this case, the H_2TMPyP molecules can be considered an electron transport mediator within the MPS nano-cavities, judging from the fact that no P(-II)H_4 was formed in a non-hydroxylic solvent. Indeed, little photocurrent was observed for the normally stacked (MV^{2+}–TNS)/(MPS) or half-stacked (MPS) hybrid films without H_2TMPyP [42].

3.2.2. Photoreactions for V_a = −0.4 V

Changes in the differential absorption spectral of the (MV^{2+}–TNS)/(H_2TMPyP–MPS) hybrid films under UV-light irradiation with an applied voltage of (V_a) = −0.4 V in acetonitrile are

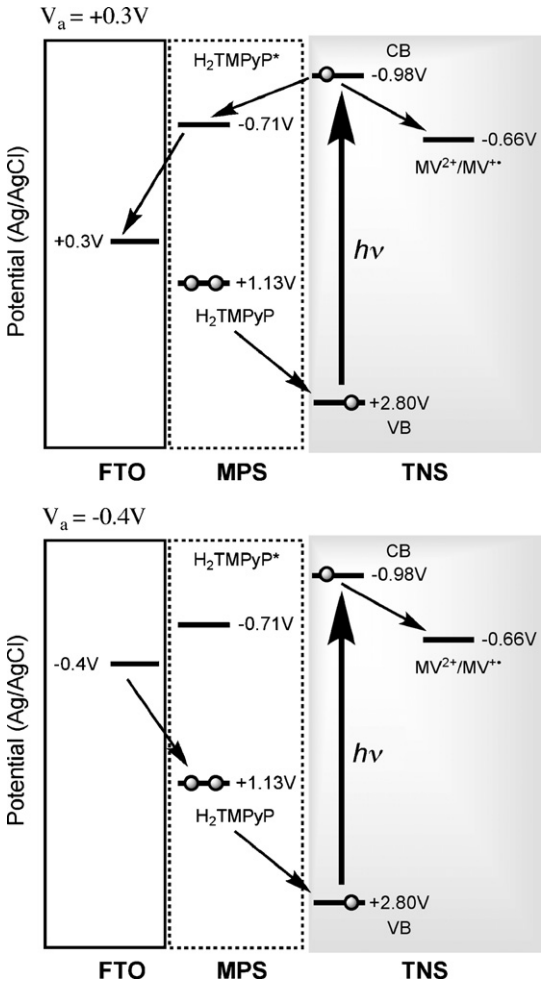

Scheme 3. Proposed schemes for the electron flow in the normally stacked (MV^{2+}–TNS)/(H_2TMPyP–MPS) hybrid films on a FTO electrode in acetonitrile solution with applied positive (+0.3 V) and negative (−0.4 V) bias voltages.

shown in Fig. 5b. The consumption of H_2TMPyP was synchronized with the formation $MV^{+\bullet}$, however, its reduced species, P(-II)H_4, was not formed by UV-light irradiation. In contrast to the positive bias voltage (+0.3 V), a considerable amount of cathodic photocurrent was generated (Fig. 5b, inset), suggesting that the reduction of MV^{2+} in TNS may be preferential to that of H_2TMPyP. Photochemically generated e_{cb}^- may reduce the MV^{2+} molecules in TNS and, at the same time, h^+ may oxidize H_2TMPyP into $[H_2TMPyP]_{ox}$ in MPS, generating anodic currents due to the electron flow from the FTO electrode to the $[H_2TMPyP]_{ox}$.

On the basis of these observations, the proposed electron migration mechanisms for the normally stacked (MV^{2+}–TNS)/(H_2TMPyP–MPS) hybrid films in CH_3CN are shown in Scheme 3. These results validate the series of proposed reaction mechanisms for the reduction of MV^{2+} in TNS, the oxidation of H_2TMPyP in MPS, the electron migrations through the interface, and the formation of photo-induced charge separated (CS) states within the (MV^{2+}–TNS)/(H_2TMPyP–MPS) hybrid films, as shown in Eqs. (1)–(3).

3.3. The inversely stacked (H_2TMPyP–MPS)/(TNS) films: in H_2O

The photo-generated e_{cb}^- was efficiently trapped by the H_2TMPyP in the MPS nano-cavities, judging from the fact that neither $[H_2TMPyP]_{ox}$ nor $MV^{+\bullet}$ could be formed in aqueous solutions. The inversely stacked (H_2TMPyP–MPS)/(TNS) hybrid films were

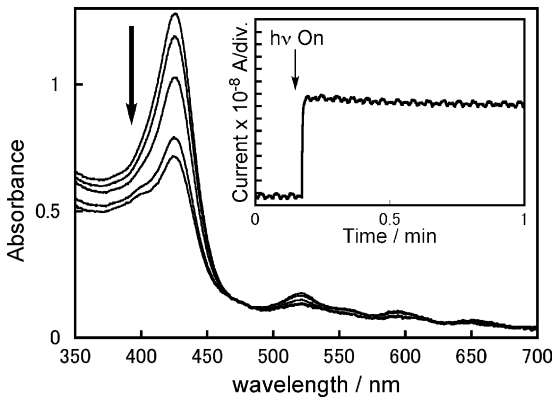

Fig. 6. Changes in the absorption spectra for the inversely stacked (H_2TMPyP–MPS)/(TNS) hybrid films on a FTO electrode by UV-light irradiation of 0–300 min in aqueous solution with: (a) a positive (+ 0.3 V) applied voltage. Inset shows the photocurrents generated with the inversely stacked (H_2TMPyP–MPS)/(TNS) hybrid films on the FTO electrode.

synthesized for the enhancement of the electron migration and CS state in the interface of MPS and TNS. Here, the H_2TMPyP–MPS film was put on TNS/FTO which was prepared by casting the TNS film on the FTO electrode and these were noted to be directly attached in the hybrid film. Since the generated e_{cb}^- are trapped by the FTO electrodes, the remaining h^+ may efficiently oxidize the H_2TMPyP in the nano-cavities, even in water.

The changes in the absorption spectra and photocurrent generation in the inversely stacked (H_2TMPyP–MPS)/(TNS) hybrid films under conditions of V_a = +0.3 V are shown in Fig. 6. Upon UV-light irradiation of the inversely stacked films, a monotonic decrease in the Soret bands was observed accompanied by the generation of considerable anodic currents, though no new absorption bands appeared in visible regions. These results suggest that the e_{cb}^- were efficiently trapped by the FTO electrode, inducing h^+ oxidation of H_2TMPyP in the MPS nano-cavities of the inversely stacked (H_2TMPyP–MPS)/(TNS) hybrid films, as shown in Scheme 4. Table 2 compares the amounts of the oxidative consumption of the H_2TMPyP molecules with those of the anodic photocurrents in the MPS nano-cavities for the inversely stacked (H_2TMPyP–MPS)/(TNS) hybrid films for the initial 1 min of light irradiation as well as

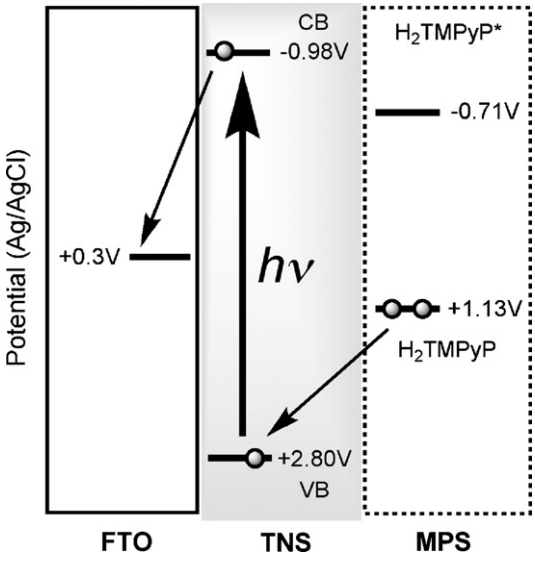

Scheme 4. Proposed schemes of the electron flow in the inversely stacked (H_2TMPyP–MPS)/(TNS) hybrid films on a FTO electrode in H_2O with an applied bias voltage of +0.3 V.

Table 2
Comparison of amount of H_2TMPyP consumption with anodic photocurrents.

Reactions	Irradiation time	
	1 min	300 min
H_2TMPyP Consumption (mol[a])	4.0×10^{-11}	5.1×10^{-9}
Photocurrent (e^-)	4.5×10^{-11}	10.2×10^{-9}
Photocurrent (C)	4.3×10^{-6}	9.8×10^{-4}

[a] Estimated by absorbance changes in the Soret bands shown in Fig. 6.

continuous irradiation for 300 min. In the case of a short irradiation time of 1 min, most of the anodic photocurrents, i.e., *ca.* 90%, could be used for the oxidative consumption of H_2TMPyP. Moreover, in the case of continuous irradiation for 300 min, the photocurrents decreased exponentially, presumably since e^-_{cb} tends to recombine with h^+ within the TNS sheets before oxidation of the H_2TMPyP in the MPS nano-cavities due to a decrease in the concentration of H_2TMPyP. Hence, it was seen that only 50% of the H_2TMPyP molecules were oxidized by amount of photocurrents generated.

4. Summary

Two different types of hybrid films, i.e., a normally stacked (MV^{2+}–TNS)/(H_2TMPyP–MPS) film and an inversely staked (H_2TMPyP–MPS)/(TNS) film, were successively stacked on a FTO electrode and their characteristic photo-induced electron transfer through the TNS/MPS interfaces were investigated. Absorption measurements clearly showed that the H_2TMPyP molecules were accommodated only in the MPS nano-cavities for both the normally and inversely stacked films, and not intercalated within the interlayers of TNS.

In the case of the normally stacked (MV^{2+}–TNS)/(H_2TMPyP–MPS) film in aqueous solution, anodic photocurrents were generated, accompanied by the formation of two electron-reduced porphyrins (P(-II)H_4) upon UV-light irradiation. With this hybrid film, such behavior was independent of the applied bias voltage (V_a). In contrast, for the normally stacked films in CH_3CN, anodic and cathodic photocurrents were observed by applying a positive and negative bias voltage, respectively. Interestingly, little photocurrent was generated when there were no H_2TMPyP in the MPS nano-cavities, suggesting the intervention of the H_2TMPyP as an electron donor and mediator in the hybrid (MV^{2+}–TNS)/(H_2TMPyP–MPS) films.

The inversely stacked (H_2TMPyP–MPS)/(TNS) films without MV^{2+} as electron acceptors exhibited characteristic anodic photocurrents with the disappearance of H_2TMPyP. This suggests that the photo-generated e^-_{cb} in TNS was trapped by the FTO electrode, whereas the h^+ oxidized the H_2TMPyP in the MPS nano-cavities. The absorption spectral changes were quite similar to those for the normally stacked (MV^{2+}–TNS)/(H_2TMPyP–MPS) films under air [35]. Based on the above results, the electron/holes in these hybrid films were concluded to migrate through the interface of TNS/MPS by the processes outlined in Eqs. (1)–(3). The products eventually detected by the present photo-induced electron flow were the one-electron reduced MV^{2+} (i.e., $MV^{+\bullet}$) and oxidized H_2TMPyP (*i.e.*, $H_2TMPyP^{+\bullet}$), which separately appeared in the TNS layers and MPS cavities of the (MV^{2+}–TNS)/(H_2TMPyP–MPS) films, respectively.

The mechanism for the present unique photo-induced electron flow in the hybrid films at the molecular levels is considered as follows: (1) Diffusion or migration of the dye molecules in the hybrid films; (2) Electron/hole hopping between the H_2TMPyP in the MPS nano-cavities; and (3) The photo- or electric-activities of the MPS films. There is less possibility of the molecular diffusion of the MV^{2+} and H_2TMPyP molecules assisting the electron flows in the hybrid films, as they are adsorbed electrostatically on the surface of the inorganic host materials.

The porphyrin molecules are homogeneously dispersed in the entire surface of the MPS films on the basis of area-selected elemental analysis using energy dispersive spectroscopy (EDS) [38], and at the same time, they exist in non-aggregated form judging from their characteristic absorption spectra. By comparisons between the surface area of MPS and the adsorbed amounts of the H_2TMPyP molecules, the average unit area and intermolecular distance were estimated to be 2900 nm^2 and *ca.* 54 nm, respectively [35]. These results indicate that there is little possibility of electron/hole hopping among the adjacent H_2TMPyP molecules since the H_2TMPyP molecules are spatially isolated and homogeneously dispersed in the MPS nano-cavities.

Under the present irradiation conditions, the MPS films can be said to exhibit little photocatalytic activity since no photocurrent generation (<1 nA) for the MPS film alone, i.e., without H_2TMPyP. This is in stark contrast to the photocurrent generation of *ca.* 80 nA in the case of single-coated H_2TMPyP–MPS films on an FTO electrode [42]. These results clearly indicate no direct photocurrent generation from the MPS films.

Judging from these results, the electron flow at the molecular level yet remains unclear, however, the following possibilities can be considered: (I) The silica-like MPS should be basically inert for various organic reactions, however, the catalytic activities or semiconductor-like functions of SiO_2 have been reported by various researchers [47–50]. Oxygen defects or lone-pair of oxygen atoms in SiO_2 is suggested to play an important role in the photocatalytic activities. There is the possibility that the oxygen or oxygen defects may assist the hole migrations in the MPS nano-cavities of the present (MV^{2+}–TNS)/(H_2TMPyP–MPS) hybrid system; (II) Nogami et al. have observed the proton-mediated conductivity of sol–gel silica glass or MPS derivatives and proposed proton conductivity with the sol–gel silica glass or MPS derivatives, exhibiting the possibility of proton migration through the OH of the silanol group on the MPS surface [51]. A similar proton conductive nature is likely to play a role in the hole migrations of these hybrid systems; and (III) Tatsuma et al. have reported the remote photocatalytic oxidation of organic molecules by stable, photochemically generated H_2O_2 from TiO_2 [52]. The formation and dispersion of H_2O_2 may assist in the oxidation of H_2TMPyP in MPS. Further investigations on the electron flow pathways within the MPS nano-cavities are now underway.

The present hybrid system is interesting for the electron/hole migration through photo- and electrochemically inert MPS films, one of the key elements in the development of photo-functional devices such as capacitors and triggers for chemical reactions as well as the construction of Z-scheme type modules for photosynthetic reactions in solar energy storage systems.

Acknowledgements

The authors are deeply grateful to the reviewers for their valuable suggestions. This work was partly supported by the KAKENHI Fund (Grant-in-Aid for Science Research) on Priority Area Research, "Strong Photon-Molecule Coupling Fields (No. 470)" (No. 19049009 and 20043029) of the Ministry of Education, Culture, Sports, Science and Technology of Japan.

References

[1] (a) T. Yui, K. Takagi, in: K. Ariga, H.S. Nalwa (Eds.), Bottom-Up Nanofabrication, American Scientific Publishers, in press (Chapter 61).;
(b) R. Sasai, T. Yui, K. Takagi, in: H.S. Nalwa (Eds.), Encyclopedia of Nanoscience, American Scientific Publishers, in press;
(c) T. Yui, K. Takagi, J. Soc. Photogr. Sci. Technol. Jpn. 66 (2003) 326.
[2] (a) M. Ogawa, K. Kuroda, Chem. Rev. 95 (1995) 399;
(b) S. Takagi, M. Eguchi, D.A. Tryk, H. Inoue, J. Photochem. Photobiol. C 7 (2006) 104;
(c) J.K. Thomas, Chem. Rev. 105 (2005) 1683.

[3] K. Kuroda, T. Sasaki (Eds.), Science and Applications of Inorganic Nanosheets, CMC Publishers, Tokyo, 2005 (in Japanese).
[4] (a) V. Ramamurthy, J. Photochem. Photobiol. C 1 (2000) 145;
(b) J.V. Smith, Chem. Rev. 88 (1988) 149.
[5] (a) K. Takagi, T. Shichi, in: V. Ramamurthy, K. Schanze (Eds.), Solid State and Surface Photochemistry, vol. 5, Marcel Dekker, New York, 2000, p. 31;
(b) T. Shichi, K. Takagi, J. Photochem. Photobiol. C 1 (2000) 113;
(c) J. Bujdak, Appl. Clay Sci. 34 (2006) 58;
(d) S.L. Suib, Chem. Rev. 93 (1993) 803;
(e) J.K. Thomas, Chem. Rev. 93 (1993) 301.
[6] (a) T. Yui, H. Yoshida, H. Tachibana, D.A. Tryk, H. Inoue, Langmuir 18 (2002) 891;
(b) R.H.A. Ras, Y. Umemura, C.T. Johnston, A. Yamagishi, R.A. Schoonheydt, Phys. Chem. Chem. Phys. 9 (2007) 918;
(c) T. Yui, T. Kameyama, T. Sasaki, T. Torimoto, K. Takagi, J. Porphyrins Phthalocyanines 11 (2007) 428;
(d) I. Shindachi, H. Hanaki, R. Sasai, T. Shichi, T. Yui, K. Takagi, Res. Chem. Intermed. 33 (2007) 143;
(e) S. Takagi, M. Eguchi, T. Yui, H. Inoue, Clay Sci. 12 (2006) 82;
(f) R. Matsuoka, T. Yui, R. Sasai, K. Takagi, H. Inoue, Mol. Cryst. Liq. Cryst. 341 (2000) 1137.
[7] K. Lang, P. Bezdicka, J.L. Bourdelande, J. Hernando, I. Jirka, E. Kafunkova, F. Kovanda, P. Kubat, J. Mosinger, D.M. Wagnerova, Chem. Mater. 19 (2007) 3822.
[8] (a) A. Corma, Chem. Rev. 97 (1997) 2373;
(b) M. Ogawa, J. Photochem. Photobiol. C 3 (2002) 129;
(c) S. Angelos, E. Johansson, J.F. Stoddart, J.I. Zink, Adv. Funct. Mater. 17 (2007) 2261;
(d) K. Ariga, A. Vinu, J.P. Hill, T. Mori, Coord. Chem. Rev. 251 (2007) 2562;
(e) E. Johansson, E. Choi, S. Angelos, M. Liong, J.I. Zink, J. Sol–Gel Sci. Technol. 46 (2008) 313;
(f) Y. Yamauchi, M. Sawada, M. Komatsu, A. Sugiyama, T. Osaka, N. Hirota, Y. Sakka, K. Kuroda, Chem. Asian J. 2 (2007) 1505.
[9] (a) D.M. Kaschak, J.T. Lean, C.C. Waraksa, G.B. Saupe, H. Usami, T.E. Mallouk, J. Am. Chem. Soc. 121 (1999) 3435;
(b) H. Hata, Y. Kobayashi, V. Bojan, W.J. Youngblood, T.E. Mallouk, Nano Lett. 8 (2008) 794;
(c) P.G. Hoertz, T.E. Mallouk, Inorg. Chem. 44 (2005) 6828 (and references therein).
[10] (a) T. Itoh, I. Matsubara, W. Shin, N. Izu, Mater. Lett. 61 (2007) 4031;
(b) T. Itoh, I. Matsubara, W. Shin, N. Izu, Chem. Lett. 36 (2007) 100;
(c) T. Itoh, I. Matsubara, W. Shin, N. Izu, M. Nishibori, Bull. Chem. Soc. Jpn. 81 (2008) 1331;
(d) E. Brunet, M. Alonso, M.C. Quintana, P. Atienzar, O. Juanes, J.C. Rodriguez-Ubis, H. Garcia, J. Phys. Chem. C 112 (2008) 5699;
(e) H. Sato, H.K. Okamoto, K. Tamura, H. Yamada, K. Saruwatari, T. Kogure, A. Yamagishi, Apple. Phys. Expr. 1 (2008) 0350001;
(f) S. Ida, C. Ogata, M. Eguchi, W.J. Youngblood, T.E. Mallouk, Y. Matsumoto, J. Am. Chem. Soc. 130 (2008) 7052;
(g) M. Eguchi, M.S. Angelone, H.P. Yennawar, T.E. Mallouk, J. Phys. Chem. C 112 (2008) 11280;
(h) K. Maeda, M. Eguchi, W.J. Youngblood, T.E. Mallouk, Chem. Mater. 20 (2008) 6770;
(i) H. Usami, Y. Iijima, Y. Morizumi, H. Fujimatsu, E. Suzuki, H. Inoue, Res. Chem. Intermed. 33 (2007) 101;
(k) R. Ma, Y. Kobayashi, W.J. Youngblood, T.E. Mallouk, J. Mater. Chem. 18 (2008) 5982 (and references therein).
[11] (a) H. Sato, A. Yamagishi, J. Photochem. Photobiol. C 8 (2007) 67;
(b) F.L. Arbeloa, V.M. Martinez, T.A. Lopez, I.L. Arbeloa, J. Phtochem. Photobiol. C 8 (2007) 85.
[12] (a) K. Takagi, T. Shichi, H. Usami, Y. Sawaki, J. Am. Chem. Soc. 115 (1993) 4339;
(b) R. Sasai, N. Shin'ya, T. Shichi, K. Takagi, Langmuir 15 (1999) 413;
(c) T. Itoh, T. Shichi, T. Yui, K. Takagi, Langmuir 21 (2005) 3217;
(d) T. Itoh, M. Yamashita, T. Shichi, T. Yui, K. Takagi, Chem. Lett. 34 (2005) 990;
(e) T. Itoh, T. Shichi, T. Yui, K. Takagi, J. Colloid Interface Sci. 291 (2005) 218;
(f) T. Itoh, N. Ohta, T. Shichi, T. Yui, K. Takagi, Langmuir 19 (2003) 9120.
[13] (a) S. Takagi, T. Shimada, M. Eguchi, T. Yui, H. Yoshida, D.A. Tryk, H. Inoue, Langmuir 18 (2002) 2265;
(b) S. Takagi, T. Shimada, T. Yui, H. Inoue, Chem. Lett. 30 (2001) 128.
[14] (a) M. Eguchi, S. Takagi, H. Tachibana, H. Inoue, J. Phys. Chem. Solids 65 (2004) 403;
(b) M. Eguchi, S. Takagi, H. Inoue, Chem. Lett. 35 (2006) 14;
(c) M. Eguchi, H. Tachibana, S. Takagi, D.A. Tryk, H. Inoue, Bull. Chem. Soc. Jpn. 80 (2007) 1350.
[15] T. Yui, S.R. Uppili, T. Shimada, H. Yoshida, D.A. Tryk, H. Inoue, Langmuir 18 (2002) 4232.
[16] (a) T. Itoh, K. Yano, Y. Inada, Y. Fukushima, J. Am. Chem. Soc. 124 (2002) 13437;
(b) T. Itoh, K. Yano, T. Kajino, S. Itoh, Y. Shibata, H. Mino, R. Miyamoto, Y. Inada, S. Iwai, Y. Fukushima, J. Phys. Chem. B 108 (2004) 13683;
(c) I. Oda, K. Hirata, S. Watanabe, Y. Shibata, T. Kajino, Y. Fukushima, S. Iwai, S. Itoh, J. Phys. Chem. B 110 (2006) 1114.
[17] (a) H. Ikeda, T. Minegishi, T. Miyashi, P.S. Lakkaraju, R.R. Sauers, H.D. Roth, J. Phys. Chem. B 109 (2005) 2504;
(b) H. Ikeda, T. Nomura, K. Akiyama, M. Oshima, H.D. Roth, S. Tero-Kubota, T. Miyashi, J. Am. Chem. Soc. 127 (2005) 14497.
[18] (a) V. Ramamurthy, J.V. Caspar, D.R. Corbin, J. Am. Chem. Soc. 113 (1991) 594;
(b) H. Garcia, H.D. Roth, Chem. Rev. 102 (2002) 3947 (and references therein).
[19] (a) L.A. Vermeulen, M.E. Thompson, Nature 358 (1992) 656;
(b) R.M. Krishna, V. Kurshev, L. Kevan, Phys. Chem. Chem. Phys. 1 (1999) 2833.
[20] (a) T. Nakato, K. Kuroda, C. Kato, Catal. Today 16 (1993) 471;
(b) T. Nakato, K. Kuroda, C. Kato, Chem. Mater. 4 (1992) 128;
(c) N. Miyamoto, Y. Yamada, S. Koizumi, T. Nakato, Angew. Chem. 119 (2007) 4201; Angew. Chem. Int. Ed. 46 (2007) 4123 (and references therein).
[21] N. Miyamoto, K. Kuroda, M. Ogawa, J. Phys. Chem. B 108 (2004) 4268.
[22] T. Yui, Y. Mori, T. Tsuchino, T. Itoh, T. Hattori, Y. Fukushima, K. Takagi, Chem. Mater. 17 (2005) 206.
[23] (a) S. Takagi, M. Eguchi, D.A. Tryk, H. Inoue, Langmuir 22 (2006) 1406;
(b) S. Takagi, D.A. Tryk, H. Inoue, J. Phys. Chem. B 106 (2002) 5455;
(c) S. Takagi, M. Eguchi, H. Inoue, Res. Chem. Intermed. 33 (2007) 177.
[24] L. Lu, R.M. Jones, D. McBranch, D.G. Whitten, Langmuir 18 (2002) 7706.
[25] (a) Y. Yamaguchi, T. Yui, S. Takagi, T. Shimada, H. Inoue, Chem. Lett. 30 (2001) 644;
(b) Y. Inui, T. Yui, T. Itoh, K. Higuchi, T. Seki, K. Takagi, J. Phys. Chem. B 111 (2007) 12162;
(c) T. Hattori, Y. Sugito, T. Yui, K. Takagi, Chem. Lett. 34 (2005) 1074;
(d) T. Hattori, Z. Tong, Y. Kasuga, Y. Sugito, T. Yui, K. Takagi, Res. Chem. Intermed. 32 (2006) 653.
[26] (a) M.A. Bizeto, V.R.L. Constantino, Mater. Res. Bull. 39 (2004) 1729;
(b) M.A. Bizeto, V.R.L. Constantino, Mater. Res. Bull. 39 (2004) 1811;
(c) M.A. Bizeto, W.A. Alves, C.A.S. Barbosa, A.M.D.C. Ferreira, V.R.L. Constantino, Inorg. Chem. 45 (2006) 6214;
(d) A. Furube, T. Shiozawa, A. Ishikawa, A. Wada, K. Domen, C. Hirose, J. Phys. Chem. B 106 (2002) 3065;
(e) R. Kaito, K. Kuroda, M. Ogawa, J. Phys. Chem. B 107 (2003) 4043.
[27] (a) T. Nakato, J. Sugawara, Bull. Chem. Soc. Jpn. 80 (2007) 2451;
(b) T. Nakato, S. Hashimoto, Chem. Lett. 36 (2007) 1240;
(c) T. Nakato, D. Sakamoto, K. Kuroda, C. Kato, Bull. Chem. Soc. Jpn. 65 (1992) 322;
(d) Q. Wei, K. Nakamura, Y. Endo, M. Kameyama, T. Nakato, Chem. Lett. 37 (2008) 152;
(e) Q. Wei, T. Nakato, Microporous Mesoporous Mater. 96 (2006) 84.
[28] T. Sasaki, J. Ceram. Soc. Jpn. 115 (2007) 9 (and references therein).
[29] (a) T. Sasaki, M. Watanabe, J. Am. Chem. Soc. 120 (1998) 4682;
(b) N. Sakai, K. Fukuda, T. Shibata, Y. Ebina, K. Takada, T. Sasaki, J. Phys. Chem. B 110 (2006) 6198;
(c) K. Fukuda, Y. Ebina, T. Shibata, T. Aizawa, I. Nakai, T. Sasaki, J. Am. Chem. Soc. 129 (2007) 202;
(d) Y. Umemura, E. Shinohara, A. Koura, T. Nishioka, T. Sasaki, Langmuir 22 (2006) 3870.
[30] K. Saruwatari, H. Sato, T. Kogure, T. Wakayama, M. Iitake, K. Akatsuka, M. Haga, T. Sasaki, A. Yamagishi, Langmuir 22 (2006) 10066.
[31] (a) K. Akatsuka, Y. Ebina, M. Muramatsu, T. Sato, H. Hester, D. Kumaresan, R.H. Schmehl, T. Sasaki, M. Haga, Langmuir 23 (2007) 6730;
(b) M. Muramatsu, K. Akatsuka, Y. Ebina, K. Wang, T. Sasaki, T. Ishida, K. Kiyake, M. Haga, Langmuir 21 (2005) 6590.
[32] N. Sakai, Y. Ebina, K. Takada, T. Sasaki, J. Am. Chem. Soc. 126 (2004) 5851.
[33] (a) W. Sugimoto, K. Ohuchi, Y. Murakami, Y. Takasu, Bull. Chem. Soc. Jpn. 78 (2005) 633;
(b) H. Cui, M. Zayat, D. Levy, Chem. Lett. 36 (2007) 144;
(c) S. Ida, C. Ogata, T. Inoue, K. Izawa, U. Unal, O. Altuntasoglu, Y. Matsumoto, Chem. Lett. 36 (2007) 158.
[34] (a) A. Fujishima, K. Honda, Nature 238 (1972) 37;
(b) A. Fujishima, K. Hashimoto, T. Watanabe, TiO_2 Photocatalysis: Fundamentals and Applications, BKC, Inc., Tokyo, 1999;
(c) X. Chen, S.S. Mao, Chem. Rev. 107 (2007) 2891;
(d) A. Fujishima, T.N. Rao, D.A. Tryk, J. Photochem. Photobiol. C: Photochem. Rev. 1 (2000) 1;
(e) T. Tachikawa, M. Fujitsuka, T. Majima, J. Phys. Chem. C 111 (2007) 5259 (and references therein).
[35] (a) T. Yui, T. Tsuchino, T. Itoh, M. Ogawa, Y. Fukushima, K. Takagi, Langmuir 21 (2005) 2644;
(b) T. Yui, T. Tsuchino, K. Akatsuka, A. Yamauchi, Y. Kobayashi, T. Hattori, M. Haga, K. Takagi, Bull. Chem. Soc. Jpn. 79 (2006) 386.
[36] T. Yui, Y. Kobayashi, Y. Yamada, T. Tsuchino, K. Yano, T. Kajino, Y. Fukushima, T. Torimoto, H. Inoue, K. Takagi, Phys. Chem. Chem. Phys. 8 (2006) 4585.
[37] T. Tachikawa, T. Yui, M. Fujitsuka, K. Takagi, T. Majima, Chem. Lett. 34 (2005) 1522.
[38] T. Yui, T. Kajino, T. Tsuchino, K. Okazaki, T. Torimoto, Y. Fukushima, K. Takagi, Trans. Mater. Res. Soc. Jpn. 32 (2007) 449.
[39] (a) T. Yui, N. Yamada, T. Kajino, Y. Fukushima, K. Takagi, Japanese Patent; Toku-Kai 2006-310380 (2006);
(b) T. Yui, T. Tsuchino, K. Takagi, Photoinduced electron transfer between porphyrins and viologenes in layered metal semiconductor/mesoporous silica hybrid films, Abstract of 13th Clay International Conference, 13th ICC, Tokyo, Japan, 2005, p. 75;
(c) T. Yui, T. Tsuchino, H. Mino, S. Itoh, Y. Fukushima, T. Kajino, K. Takagi, in preparation.
[40] (a) M. Ogawa, N. Masukawa, Microporous and Mesoporous Materials 38 (2000) 35;
(b) J.Y. Bae, O.-H. Park, J.-I. Jung, K.T. Ranjit, B.S. Bae, Microporous Mesoporous Mater. 67 (2004) 265.
[41] (a) Y. Yamada, T. Nakamura, K. Yano, Langmuir 24 (2008) 2779;
(b) K. Yano, T. Nakamura, Chem. Lett. 35 (2006) 1014;

(c) Y. Yamada, T. Nakamura, M. Ishii, K. Yano, Langmuir 22 (2006) 2444;
(d) Y. Yamada, K. Yano, Microporous Mesoporous Mater. 93 (2006) 190.
[42] T. Hirano, T. Yui, K. Okazaki, T. Kajino, Y. Fukushima, H. Inoue, T. Torimoto, K. Takagi, J. Nanosci. Nanotechnol. 9 (2009) 495.
[43] (a) L.A. Lucia, T. Yui, R. Sasai, H. Yoshida, S. Takagi, K. Takagi, D.G. Whitten, H. Inoue, J. Phys. Chem. B 107 (2003) 3789;
(b) L. A. Lucia, H. Inoue, T. Yui, R. Sasai, S. Takagi, K. Takagi, H. Yoshida, D.G. Whitten, Abstracts of Papers of the American Chemical Soc. 231, 109-Cell, March 26, 2006;
(c) A. Ceklovsky, A. Czimerova, M. Pentrak, J. Bujdak, J. Colloid Interface Sci. 324 (2008) 240.
[44] (a) V.G. Kuykendall, J.K. Thomas, Langmuir 6 (1990) 1350;
(b) Z. Chernia, D. Gill, Langmuir 15 (1999) 1625.
[45] H. Yao, S. Kobayashi, K. Kimura, Chem. Lett. 37 (2008) 594.
[46] B.P. Neri, G.S. Wilson, Anal. Chem. 44 (1972) 1002.
[47] (a) Y. Sakata, M.A. Uddin, A. Muto, K. Koizumi, Y. Kanda, K. Murata, J. Anal. Appl. Pyrolysis 43 (1997) 15;
(b) J. Haber, K. Pamin, L. Matachowski, D. Mucha, Appl. Catal. A 256 (2003) 141;
(c) T. Yamamoto, T. Tanaka, S. Inagaki, T. Funabiki, S. Yoshida, J. Phys. Chem. B 103 (1999) 6450;
(d) K. Vikulov, G. Martra, S. Collucia, D. Miceli, F. Arena, A. Parmaliana, E. Paukshtis, Catal. Lett. 37 (1996) 235 (and references therein).
[48] L. Yuliati, M. Tsubota, A. Satsuma, H. Itoh, H. Yoshida, J. Catal. 238 (2006) 214 (and references therein).
[49] (a) Y. Kato, H. Yoshida, T. Hattori, Chem. Commun. (1998) 2389;
(b) H. Yoshida, M.G. Chaskar, Y. Kato, T. Hattori, J. Photochem. Photobiol. A 160 (2003) 47;
(c) L. Yuliati, T. Hattori, H. Yoshida, Phys. Chem. Chem. Phys. 7 (2005) 195;
(d) A. Ogata, A. Kazusaka, M. Enyo, J. Phys. Chem. 90 (1986) 5201;
(e) Y. Inaki, H. Yoshida, T. Yoshida, T. Hattori, J. Phys. Chem. B 106 (2002) 9098 (and references therein).
[50] N. Kakegawa, T. Kondo, M. Ogawa, Langmuir 19 (2003) 3578.
[51] (a) T. Uma, M. Nogami, Anal. Chem. 80 (2008) 506;
(b) T. Uma, M. Nogami, Chem. Mater. 19 (2007) 3604;
(c) L. Xiong, J. Shi, L. Zhang, M. Nogami, J. Am. Chem. Soc. 129 (2007) 11878;
(d) T. Uma, M. Nogami, J. Phys. Chem. C 111 (2007) 16635 (and references therein).
[52] W. Kubo, T. Tatsuma, J. Am. Chem. Soc. 128 (2006) 16034.